Scientific Research Publishing

Open Journal of Antennas and Propagation, 2023, 11, 11-25
https://www.scirp.org/journal/ojapr
ISSN Online: 2329-8413
ISSN Print: 2329-8421

A Review on Conductive and Transparent Materials Used in the Design of Transparent Antennas

Abdoulaye Sissoko, Cheick Oumar Sanogo, Badié Diourté

Université des Sciences des Techniques et des Technologies de Bamako, Bamako, Mali
Email: abdoulaye.sissoko@isamali.org

How to cite this paper: Sissoko, A., Sanogo, C.O. and Diourté, B. (2023) A Review on Conductive and Transparent Materials Used in the Design of Transparent Antennas. *Open Journal of Antennas and Propagation*, **11**, 11-25.
https://doi.org/10.4236/ojapr.2023.112002

Received: November 29, 2022
Accepted: April 17, 2023
Published: April 20, 2023

Abstract

In this review, we highlight the essential parameters of some transparent materials for use in the design of transparent antennas. ITO films with a sheet resistance of R_s = 10 Ω/sq and a T = 90% transmittance, we turn to materials that can be serious alternatives for ITO, such as graphene T = 97% for R_s = 60 Ω/sq and the micro-mesh metal. Wire mesh seems to be the best alternative T = 93% for R_s < 0.05 Ω/sq but there is another technique to improve the visual perception of the antenna which provides a lower resistance and a good R_s = 0.022 Ω/sq at T = 81%, this is the micrometric pitch mesh.

Keywords

Transmittance, Resistance by Square, Grid, Micrometric Mesh

1. Introduction

To achieve a transparent antenna, it is necessary to use materials with high electrical conductivity (≥10^6 S/m) and a good transmittance or optical transparency (≥70%) in the visible range (400 - 800 nm). Called transparent conductive materials (TCM), these are solids that do not absorb visible light (gap greater than 3 eV). Among the materials, transparent conductive oxides (OTC), multilayers, nanowires, graphene, metal networks can be distinguished [1]. They are characterized by three main quantities: resistance by square R_s, optical transparency T and the figure of merit FMo. Many works currently exist in this field because of their various applications: transparent electrodes for photovoltaic panels, flat screens, low-emissivity glazing, pare-brises, antistatic and/or anti-glare screens, etc. The objective of this review is to find the best transparent conductive materials with the best electrical and optical characteristics for the realization of

transparent antennas.

2. Electrical and Optical Characteristics of Some Transparent Conductive Materials Used in the Design of Transparent Antennas

The optical characteristic is obtained from transparency or optical transmission. It is usually expressed as a percentage, and defined as the ratio between the outgoing light intensity of materials I_0 and the incident light intensity I. It corresponds to the transparency ratio of the material and also depends on the wavelength incident light:

$$T = I/I_0 \tag{1}$$

The electrical characteristic is materialized by the sheet resistance expressed in Ω/square, is the ohmic resistance of a material of thickness t deposited on a square surface. It corresponds to the ratio between the resistivity ρ of the material (in Ωm) and the thickness e of the thin layer (in m):

$$R_s = \rho/t \tag{2}$$

Thus, the ohmic resistance of a line of the rectangular shape of length L and width l can be written:

$$R = \rho\frac{L}{l\cdot t} = R_s\frac{L}{l} \tag{3}$$

The compromise between optical transparency and a sheet resistance is obtained from the figure of merit: It characterizes the performance of a device:

$$F_0M = \frac{\sigma_{él}}{\sigma_{op}} = \frac{Z_0}{2R_s}\times\frac{\sqrt{T}}{1-\sqrt{T}} \tag{4}$$

With Z_0 = 377 Ω the impedance of the vacuum, $\sigma_{él}$ the electrical conductivity in continuous mode and σ_{op} the optical conductivity.

2.1. Transparent Conductive Oxides (TCOs)

The optoelectronic industry has long demanded electrodes which are at the same time optically transparent and electrically conductive. Large bandgap semiconductors with heavy metal doping have been widely investigated for these applications, is known as Transparent Conductive Oxides (TCOs). Among them, the most widely used is Indium Tin Oxide (ITO - In_2O_3:Sn). The good trade-off between low electrical resistivity and high optical transmittance in the visible range of the spectrum that can be achieved by TCOs has led to their use in many electro-optic devices such as solar cells, photo-detectors and Organic Light Emitting Diodes (OLEDs). However, highly performing TCO films require accurate control of growth conditions such as doping concentration, oxygen pressure, or substrate temperature as well as post-deposition annealing treatments carried out to improve their electrical properties. Annealing treatments are usually regarded as a potential drawback for introducing the transparent electrode deposi-

tion process into an industrial flow. Moreover, polymeric substrates or materials might not withstand the high temperatures required to improve the electrical properties of indium tin oxide (ITO) films, this being a barrier to the development of flexible devices [2].

Currently, ITO (**Figure 1**) is the dominant material used for industrial-scale TCO applications. ITO not only has excellent properties with a sheet resistance of 10 Ω/square at around 90% optical transmittance [4], but also exhibits outstanding stability and compatibility with both wet and dry device processes. However, future optoelectronics require TCF materials which are mechanically flexible, lightweight, and low fabrication cost. The growing demand for ITO due to the development of solar cells may lead to an increase in substantial cost because of the relatively rare element of indium. In addition, ITO suffers from poor mechanical flexibility [1], which suppresses its application for emerging flexible, stretchable, and wearable electronic applications. However, due to the limited reserve, and toxicity of indium, high leaf resistance, high-temperature spraying process, poor mechanical ductility, and rising price, many research efforts have focused on transparent ITO (or FTO) transparent conductors.

Presented alternatives include mainly graphene, carbon nanotubes, nanowires, metal grids and metal films [4] [5]. The alternative metal oxides can use abundant materials such as SnO_2:F, CuO_2:Al and ZnO:Al. Similar to ITO, the manufacture of these oxides requires a vacuum and/or high temperature process to achieve high transmittance and low sheet resistance [4] [6].

The transmittance of the ITO film can be approximated by:

$$T \cong \mathrm{e}^{\frac{-2t}{\delta}} \tag{5}$$

where t is the thickness of the film and δ the skin depth for the visible wavelengths given by the formula [6]:

$$\delta = \sqrt{\frac{2}{\omega\mu_0\sigma}} = \sqrt{\frac{1}{\pi f\,\mu_0\sigma}} \tag{6}$$

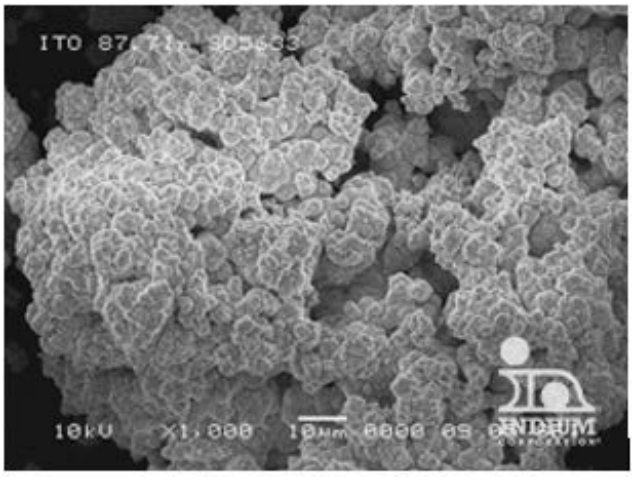

Figure 1. Indium tin oxide [3].

f is the frequency of use, σ the conductivity of the material and μ_0, the permeability of the vacuum.

An optical transparency of 85% with a sheet resistance of 2 Ω/sq for a thickness of 1100 nm was obtained with tin oxide and fluorine (SnO_2:F) [7] while for a thickness of 1000 nm of ITO, a transmittance ranging from 69% to 86% with a resistance per square of 8.6 Ω/sq was obtained. [8]. OTCs have a merit factor of 1000.

Several research groups in the last decade reported the dielectric-metal-dielectric sandwich multilayer structures as alternative to ITO [9] [10] [11].

2.2. Multilayer TCO/Metal/TCO

Multilayers have been used to reduce the ohmic resistance (R_s < 10 Ω/sq) of OTC-based layers. Intermediate metal layers Ag, Au, Cu, Al... improve flexibility. The transmittance is approximately equal to that of the ITO at room temperature with a merit factor ranging from 220 to 1500. A double multilayer ICO/Ag/ICO/Ag/ICO (**Figure 2**) has an ohmic resistance of 1.2 Ω/sq and a transmittance of 82% [8]. **Table 1** presents the electrical and optical parameters of some certain multilayers.

The square resistance R_s of the multilayer is calculated as follows:

$$\frac{1}{R_s} = \frac{1}{R_{sOTC}} + \frac{1}{R_{sMetal}} + \frac{1}{R_{sOTC}} \tag{7}$$

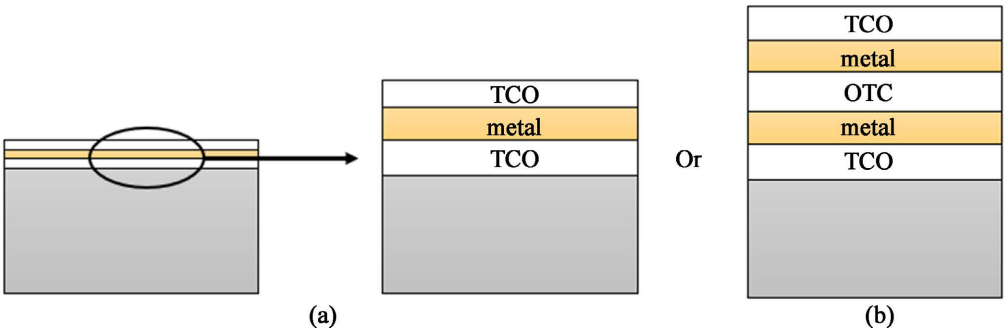

Figure 2. Diagram of (a) single multilayer TCO; (b) double multilayer.

Table 1. The values of thickness e, Sheet resistance R_s and Transmittance T of some multilayers.

Film	Film thickness (nm)	Sheet resistance(Ω/sq)	Transmittance (%) in visible spectrum	Réf
ITO/Cu/ITO	85/13/85	4.7	28 < T < 61	[8]
ZnO/Ag/ZnO	-	2.3	80%	[12]
ZnO/Ag/ZnO	30/10/30	6	90	[13]
	-	24	80	[14]
ITO/Ag/ITO	57/9/40	7	95	[13]
GZO/Ag/GZO	30/10/30	7	90.7	[13]
ITO/Au/ITO	50/10/50	4.4	75	[15]

The Ag is the best candidate with a lower absorption coefficient and refractive index in the visible. **Figure 3** shows the importance of Ag compared to Cu as an intermediate layer [16].

2.3. Ultrathin Metallic Film

Ultra-Thin Metal Films (UTMF) have proven to be a feasible alternative to TCO for transparent electrode applications. A sufficiently thin layer (a few nm to a few tens of nm) of pure metal can become optically transparent while retaining excellent electrical properties. Compared with ITO, nickel films show similar optical transmittance in the visible range, greater transparency in the ultra violet (UV) range and higher electrical conductivity [2] [17].

Ultrathin films have a very low merit factor (5 to 13) metal are unsuitable for microwave applications. A serious competitor of TCOs they have high resistivity, oxidize more easily and are mechanically fragile. They are associated with other materials to protect them. The simplest transparent and conductive material is the metal layer.

The minimum and maximum values of transmittance and sheet resistance for silver and copper layers as a function of the thickness of these films are presented on **Figure 4**. The electrical and optical parameters of some ultrathin metallic film are presented in **Table 2**.

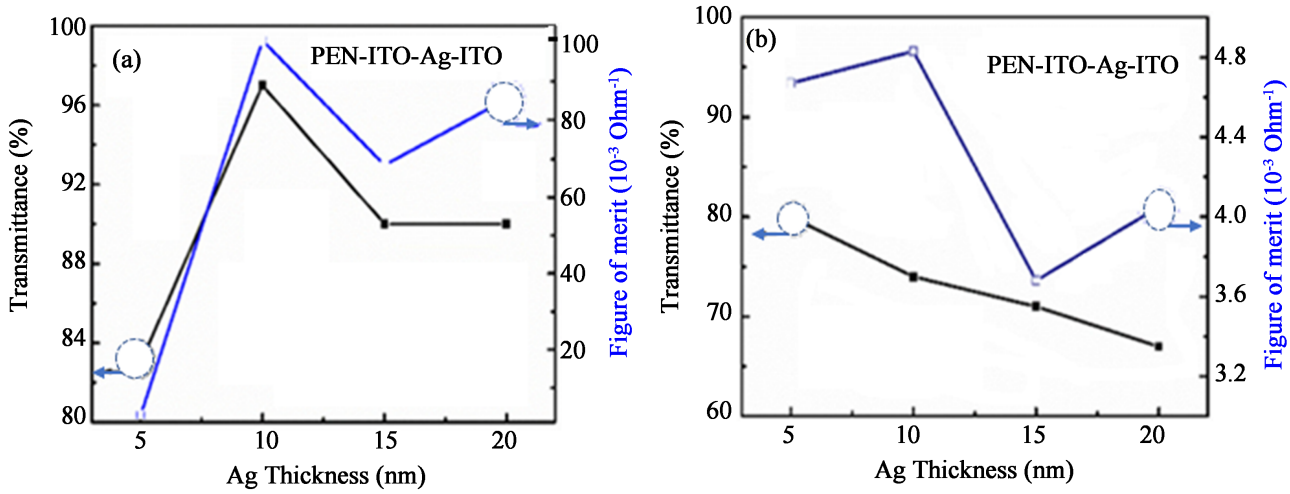

Figure 3. Transmittance at the wavelength of 550 nm and figure of merit of (a) IAgI and (b) ICuI samples as a function of the metal interlayer thickness on the PEN substrate [16].

Table 2. Film thickness, optical resistance and optical transparency in visible films.

Film	Film thickness (nm)	Sheet resistance(Ω/sq)	Transmittance (%) in visible spectrum	Ref
Ni	10	286	80	[2]
ITO	1000	8.6	69 - 86	[8]
Cu	10	8.3	45 - 64	[8] [17]
Cu	10,000	0.01	reflecting film	[17]

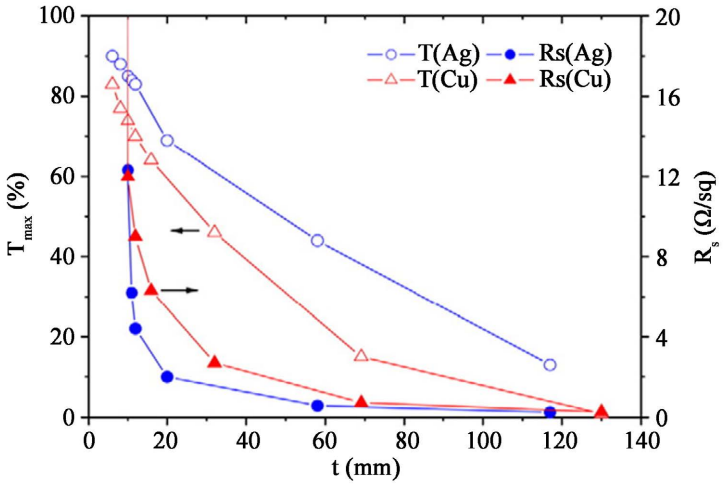

Figure 4. Representation of maximum transmittance and sheet resistance values obtained for filtered Ag and Cu coatings as a function of film thickness [13].

2.4. Graphene

Graphene has been widely studied as a promising material due to its many fascinating properties such as exceptional electronic conductivity, thermal conductivity, mechanical strength, optical transparency, and so on [18]. It has attracted interest from many potential applications. Graphene is a miracle material, the thinnest in the universe. Its charge carriers exhibit giant intrinsic mobility, have the smallest effective mass (it is zero) and can travel micro meter-long distances without scattering at room temperature.

Graphene exhibits very good electrical and optical properties in theory, and thus it can be an ideal material for transparent conductive films (TCF) application. He has a merit factor of about 210. However, the electrical properties strongly depend on the quality of graphene. The best TCFs using four or five layers of mechanically exfoliated graphene show a low leaf resistance of 8.8 Ω/square for 84% transmittance. Solution processed graphene TCFs generally show a sheet resistance of above 1000 Ω/square at a transmittance of 85% [4]. The transmittance of graphene is also outstanding at both visible [5] and terahertz (THz) frequencies, unlike the indium tin oxide (ITO) film which shows high transmittance at only visible frequencies, but very low at THz frequencies. With high chemical stability, graphene is a promising candidate as transparent electrodes [19]. Liquid crystal devices with graphene electrodes have been demonstrated at visible and near infrared frequencies. Recently, graphene has been widely studied at THz frequencies, such as graphene plasmonic structures, graphene modulators, and Dirac fermion dynamics measurements. A phase shifter at THz frequencies is an important component for applications.

The most promising efforts use graphene or ITO nanoparticle. A single layer of graphene has a high transmission capacity (>88%), but the thin layer can be difficult for the electrical connection because the resistivity of the sheet is about 230 Ω [19].

The transmittance, the square resistance and the merit factor depend on the number n of atomic monolayers and are given by:

$$T(\%) = 100 - 2.3 \cdot n \tag{8}$$

$$R_s = \frac{62.4}{n} \tag{9}$$

$$F_0 M = \frac{Z_0 n}{128.4} \times \frac{\sqrt{1 - 0.023 \cdot n}}{1 - \sqrt{1 - 0.023 \cdot n}} \tag{10}$$

An optical transparency of 97% and sheet resistance of 60 Ω/sq were measured for a monolayer (**Figure 5**) [20].

The sheet resistance and the transmission decrease with the increase in the number of layers for the multilayer graphene undoped and doped by thionyl chloride (**Figure 6**).

A sheet resistance value of 120 Ω/sq for a single layer graphene with 97.5% optical transparency was obtained by the plasma oxidation of graphene [21].

In **Table 3** Graphene added to ferric chloride ($FeCl_3$) presents the right

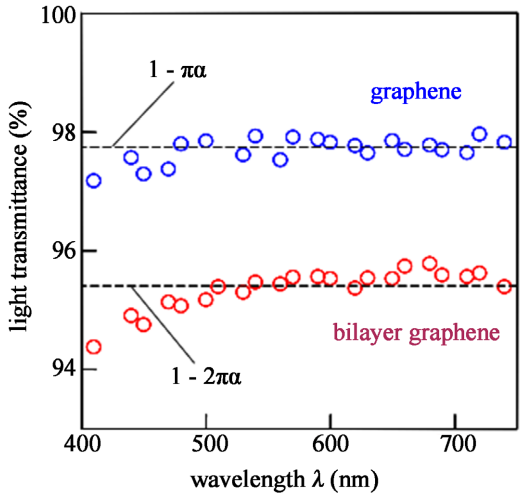

Figure 5. Transmittance spectra of monolayer and bilayer regions of the sample.

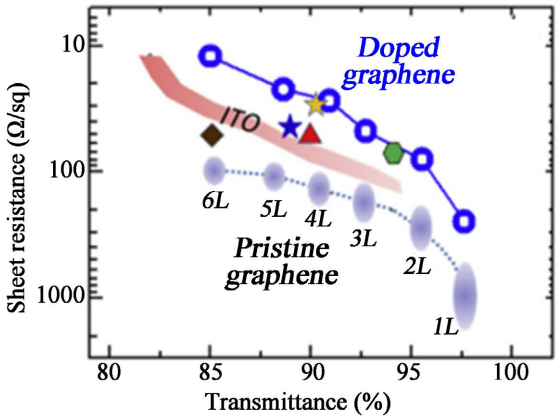

Figure 6. Sheet resistance vs Optical Transmittance for pristine and $SOCl_2$ doped single and multilayers graphene on Corning glass [21].

Table 3. Optical resistance and transparency of some types of graphene's

Graphene	R_s (Ω/sq)	T (%)	Ref
Monolayer	60	97	[20]
Multilayer	30	90	[22]
+$FeCl_3$	8.8	84	[22]
Chemically doped	125	97.7	[22]
Thin layer (difficult to achieve)	230	>88%	[23]

compromise of the sheet resistance and the transmittance.

2.5. Conductive Nanowires

Nanowires are flexible technology at low temperatures. With a merit factor ranging from 60 to 150, they exist in two forms: metallic nanowires and carbon nanotubes (CNT). Metal nanowires are becoming an effective alternative to ITO. Due to the high conductivity, transparent conductive films can be obtained from a nanoscale network of silver nanowires (Ag NWs) with a sheet resistance of 20 Ω/square for a 95% transmittance [4]. Although silver is more expensive than indium, Ag NWs offer roll-to-roll technology, which significantly reduces the overall cost of TCF series production. It has been reported that AgNW TCFs are used as touch sensors for Lenovo computers (China). However, the thermal and chemical stability of metal nanowires has yet to be studied.

Copper nanowires (Cu NW) are becoming a more promising TCF technology because copper is 100 times cheaper than silver. The best TCFs using Cu NW show a sheet resistance of 100 Ω/square for a 95% transmittance. The stability of Cu NW against oxidation is a challenge [4].

Figure 7 presents the measurements of transmission against sheet resistance of AgNWs deposited on glass substrate, on PET substrate compared with the properties of an ITO layer on glass substrate.

The transmittance of graphene, silver nanowire, carbon nanowire, carbon nanotube and silver films are shown in **Figure 8**.

The performances of technologies based on conductive nanowires are presented in **Table 4**. The hybrid solution (AgNWs + SWNTs) provides a more efficient film than the carbon nanotube but less efficient than some silver nanowires. It has a sheet resistance of 21 Ohms/square and an optical transparency of 87% giving a figure of merit of around 130.

2.6. Wire Mesh

Classically used in transparent electronic applications, the metal mesh is highly conductive since it is based on a metal structure, and allows high transparency. On the other hand, it remains visible to the naked eye since the width of the metallization's can reach 100 μm (**Figure 9**). It also has better electrical and optical performance than previous technologies, but its manufacture is more or less

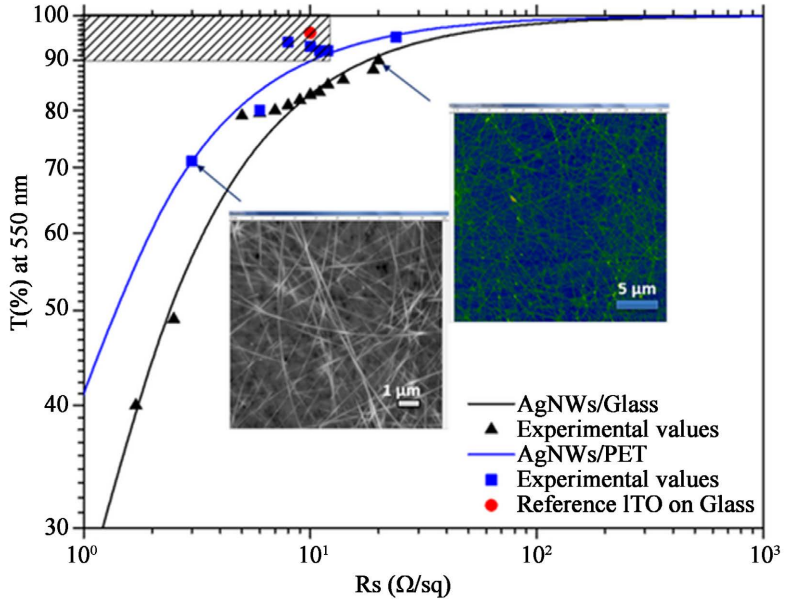

Figure 7. Measurements of transmission (T at $\lambda = 550$ nm), of the sheet resistance (R_s) of AgNWs on glass (black rectangle), on PET (blue square), and of ITO layer on glass (red dot). Solid line represents a fit of the AgNW films on glass substrate (black line) and PET substrate (blue line). Inserted optical images of AgNWs annealed at 120 ˚C, 10 min on glass and PET substrates [24].

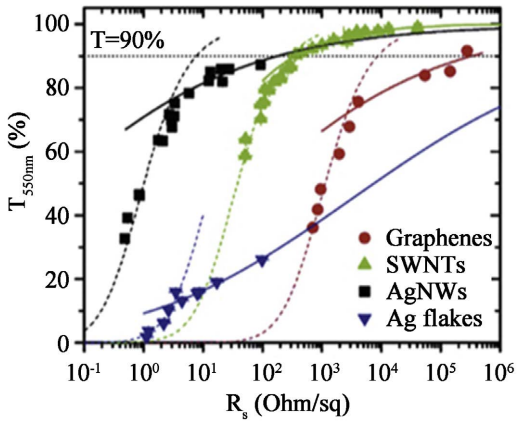

Figure 8. Transmittance (550 nm) plotted as a function of sheet resistance for thin films [25].

Table 4. Sheet resistance and transmittance of some nanowires

Nanowires	R_s (Ω/sq)	T (%)	Ref
AgNWs metal nanofilms)	13	85	[26]
	10	80	[24]
Single walled nanotube (SWNTs)	100 - 500	80 - 95	[27]
Hybrid (AgNWs + SWNTs)	21	87.5	[27]

complicated depending on the design. Transmittance is the ratio of the surface of the openings in the patch to the entire surface of the patch, it is given by the relation:

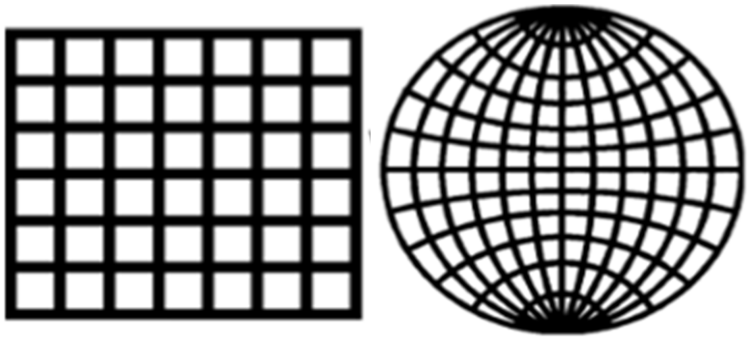

Figure 9. Meshed patch antennas (a) rectangular; (b) circular [28].

Table 5. Transparent conductive film comparison.

Material	Transparency	Sheet Resistance	Efficiency
ITO Films	90%	4.6 Ω/sq	Low
Meshed Conductors	93%	<0.05 Ω/sq	High

$$T = \frac{A_{\text{see-through}}}{A_{\text{patch}}} \times 100\% \tag{12}$$

With similar transparencies, the wire mesh has a very low resistance compared to the ITO (**Table 5**).

Wire mesh has the best merit factor: 145,000.

2.7. Micrometric Pitch Meshing

We start from the same principle as the wire mesh by reducing the width and the mesh pitch so that it is invisible to the eye and the mesh thin film appears as homogeneous. With this model, the value of R_s is reduced, R_s = 0.022 Ω/sq at T = 81% [29]. There is a merit factor of 69,000.

To define the values of the parameters of the metal mesh so that it is as transparent as possible, we use the performance of the human eye. The mesh pitch must be smaller than human visual acuity: the angle under which two points are observed must be less than $\theta_{\min} = 4.9 \times 10^{-4}$ rad [30], so that the eye is no longer able to discriminate between them (**Figure 10**). Thus, depending on the distance of the people to the mesh (the minimum distance being equal to that of vision of the near point, or Punctum Proximum, *i.e.* L = 25 cm on average), the value of the gap to manufacture these antennas corresponds to the opening G separating two points and must remain less than:

$$G_{\max} = L \cdot \tan\left(\theta_{\min}\right) \approx L \cdot \theta_{\min} \tag{12}$$

With ($\theta_{\min} = 4.9 \times 10^{-4}$ rad), L: the distance at which the eye observes the two points.

There are different calculation methods used for wire mesh and micro-pitch mesh to determine the theoretical transmittance and resistance per sheet ac-

cording to the mesh (Figure 11).

For a square mesh, the transmittance of the grid [30]:

$$T(\%) = \left(\frac{p-s}{p}\right)^2 T_{sub} \tag{13}$$

For a rectangular mesh:

$$T(\%) = \left(\frac{p_x - s_x}{p_x}\right) \times \left(\frac{p_y - s_y}{p_y}\right) \times T_{sub} \tag{14}$$

For the metallic mesh (*e:* film thickness), the resistance per square is given by:

$$R_s' = \frac{p}{s} R_s \tag{15}$$

$$F_0 M = \frac{Z_0 \times e}{2p} \times \frac{p-s}{p} \tag{16}$$

2.8. Metal Micromaillage

Considered as a new technique to have a transparent material, metallic micro-maillage a conductive film based on micro-metals (MM) nanoparticle technology

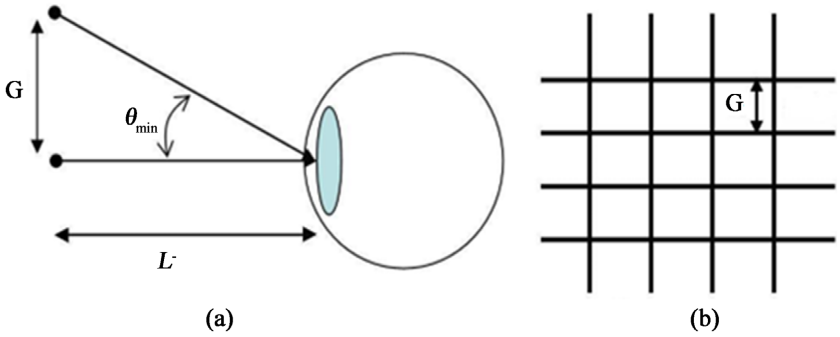

Figure 10. Principle diagram of the discrimination of two objects observed with the naked eye (a), mesh geometry (b).

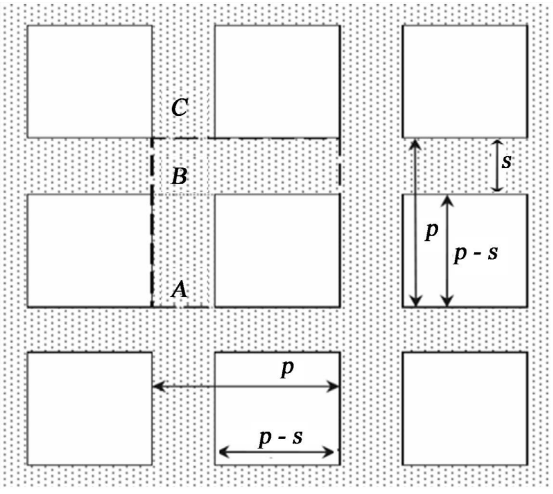

Figure 11. Mesh pattern.

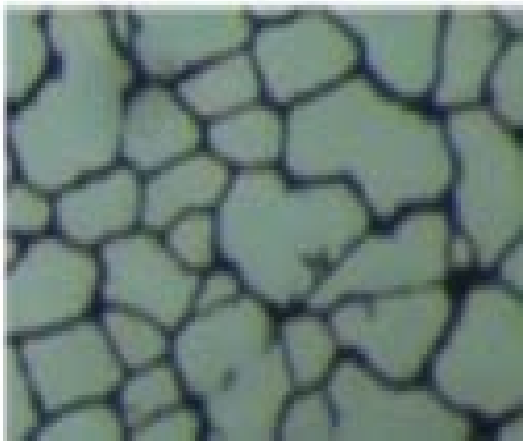

Figure 12. Transparent MM conductive film.

self-assembly, it has a very remarkable property, microwave (**Figure 12**) [31]. Not only high optical transparency, but also high electrical conductivity. It has a sheet resistance of 0.7 Ω/sq and a visible light the transmittance is 75% [32]. His merit factor equals 1700.

3. Conclusion

A certain number of technological solutions with low visual impact making it possible despite everything to ensure electrical conductivity properties comparable to those of conventional conductors were presented. Ultra-thin conductive film offers the lowest figure of merit among transparent conductive materials (less than 10), so it is not recommended for microwave applications. Conductive transparent oxides, in particular the ITO historically used as TCM, present a good compromise between resistivity and optical transparency with a figure of merit reaching 1000. On the other hand, the electrical resistance of the ITO remains high, and its implementation cost work is too high for the realization of inexpensive devices. In addition, it suffers from low mechanical flexibility. These shortcomings are improved with multi-layered OTC/metal/OTC solutions. The figure of merit increases until it reaches about 1500 but its transparency is not constant in the visible spectrum. Promising technologies such as nanowires and graphene, with figures of merit of around 1080 and 230 respectively, exhibit high resistances. Considering the characteristics and performances of the different solutions, the metal mesh seems to offer the highest figure of merit (>100,000) with a transmittance greater than 90% and a resistance per square less than 0.05 Ohm/sq. It therefore constitutes an interesting solution to synthesize optically transparent conductive materials for the design of antennas with low visual impact. Despite everything, the grids remain visible to the naked eye because of their thickness. For the deposit to appear homogeneous, the mesh with micrometric pitch, with finer grid widths, also presents a significant figure of merit (>50,000). The latter can be used to make antennas with low visual impact but with a lower transmittance compared to thick mesh.

Conflicts of Interest

The authors declare no conflicts of interest regarding the publication of this paper.

References

[1] Lu, X., Zhang, Y. and Zheng, Z. (2021) Mandal-Based Flexible Transparent Electrodes: Challenges and Recent Advances. *Advanced Electronic Materials*, **7**, Article 2001121. https://doi.org/10.1002/aelm.202001121

[2] Martinez, L., Ghosh, D.S., Giurgola, S., Vergani, P. and Pruneri, V. (2008) Utrathin Mandal Film: An Emerging Transparent Electrode for the Optoelectronics Industry. 2008 4*th International Conference on Advanced Optoelectronics and Lasers*, Alushta, 29 September-4 October 2008, 15-17. https://doi.org/10.1109/CAOL.2008.4671928

[3] Indium Compounds | Inorganic Compounds | Products made by Indium Corporation. Indium Corporation. https://www.indium.com/products/inorganic-compounds/indium-compounds/

[4] Zhou, Y. and Azumi, R. (2016) Carbon Nanotube Based Transparent Conductive Films: Progress, Challenges, and Perspectives. *Science and Technology of Advanced Materials*, **17**, 493-516. https://doi.org/10.1080/14686996.2016.1214526

[5] Chen, D., *et al.* (2018) Simulation Study toward High-Performance Transparent-Conductive-Oxide Free Perovskite Solar Cells Using Mandal Microcavity and Optical Coupling Layer. *IEEE Photonics Journal*, **10**, 1-9. https://doi.org/10.1109/JPHOT.2018.2815569

[6] Harati, M.R., Naser-Moghadasi, M., Lotfi-Neyestanak, A.A. and Nikfarjam, A. (2015) Improving the Efficiency of Transparent Antenna Using Gold Nano Layer Deposition. *IEEE Antennas and Wireless Propagation Letters*, **15**, 4-7. https://doi.org/10.1109/LAWP.2015.2424918

[7] Ching, E., Watson, A. and Miranda, H. (2018) Optical and Electrical Properties of Fluorine Doped Tin Oxide Thin Film. *Journal of Materials Science: Materials in Electronics*, **29**, 15299-15306. https://doi.org/10.1007/s10854-018-8795-8

[8] Castel, X., Himdi, M. and Colombel, F. (2018) Comparison of the Microwave Performance of Transparent Monopole Antennas Made of Different Transparent Conducting Films. 2018 *IEEE Conference on Antenna Measurements & Applications*, Vasteras, 3-6 September 2018, 1-4. https://doi.org/10.1109/CAMA.2018.8530552

[9] Sarma, B., Barman, D. and Sarma, B.K. (2019) AZO (Al:ZnO) Thin Films with High Figure of Merit as Stable Indium Free Transparent Conducting Oxide. *Applied Surface Science*, **479**, 786-795. https://doi.org/10.1016/j.apsusc.2019.02.146

[10] Chiu, P.K., Cho, W.H., Chen, H.P., Hsiao, C.N. and Yang, J.R. (2012) Study of a Sandwich Structure of Transparent Conducting Oxide Films Prepared by Electron Beam Evaporation at Room Temperature. *Nanoscale Research Letters*, **7**, Article No. 304. https://doi.org/10.1186/1556-276X-7-304

[11] Sarma, B. and Sarma, B.K. (2018) Role of Residual Stress and Texture of ZnO Nanocrystals on Electro-Optical Properties of ZnO/Ag/ZnO Multilayer Transparent Conductors. *Journal of Alloys and Compounds*, **734**, 210-219. https://doi.org/10.1016/j.jallcom.2017.11.028

[12] Chen, Z., *et al.* (2023) Analysis of the Effect of Graphene, Mandal, and Mandal Oxide Transparent Electrodes on the Performance of Organic Optoelectronic De-

vices. *Nanomaterials*, **13**, Article 25. https://doi.org/10.3390/nano13010025

[13] Guillén, C. and Herrero, J. (2011) TCO/Mandal/TCO Structures for Energy and Flexible Electronics. *Thin Solid Films*, **520**, 1-17. https://doi.org/10.1016/j.tsf.2011.06.091

[14] Sharma, V., Kumar, P., Kumar, A. Surbhi, Asokan, K. and Sachdev, K. (2017) High-Performance Radiation Stable ZnO/Ag/ZnO Multilayer Transparent Conductive Electrode. *Solar Energy Materials and Solar Cells*, **169**, 122-131. https://doi.org/10.1016/j.solmat.2017.05.009

[15] Lee, J.Y., *et al.* (2009) Dependence of Intermediated Noble Mandals on the Optical and Electrical Properties of ITO/Mandal/ITO Multilayers. *Optics Communications*, **12**, 2362-2366. https://doi.org/10.1016/j.optcom.2008.12.044

[16] Li, H., Gao, Y.J., Yuan, S.H., Wuu, D.S., Wu, W.Y. and Zhang, S. (2021) Improvement in the Figure of Merit of ITO-Mandal-ITO Sandwiched Films on Poly Substrate by High-Power Impulse Magnandron Sputtering. *Coatings*, **11**, Article 144. https://doi.org/10.3390/coatings11020144

[17] Colombel, F., Castel, X., Himdi, M., Legeay, G., Vigneron, S. and Cruz, E.M. (2009) Ultrathin Mandal Layer, ITO Film and ITO/Cu/ITO Multilayer towards Transparent Antenna. *IET Science*, *Measurement & Technology*, **3**, 229-234. https://doi.org/10.1049/iet-smt:20080060

[18] Chung, K.H., *et al.* (2014) Convection-Based Realtime Polymerase Chain Reaction (PCR) Utilizing Transparent Graphene Heaters. *SENSORS*, 2014 *IEEE*, Valencia, 2-5 Noverber, 1006-1009. https://doi.org/10.1109/ICSENS.2014.6985173

[19] Wu, Y., *et al.* (2013) Graphene/Liquid Crystal Based Terahertz Phase Shifters. *Optics Express*, **21**, 21395-21402. https://doi.org/10.1364/OE.21.021395

[20] Nair, R.R., *et al.* (2008) Fine Structure Constant Defines Visual Transparency of Graphene. *Science*, **320**, 1308-1308. https://doi.org/10.1126/science.1156965

[21] Bianco, G.V., *et al.* (2020) Extraordinary Low Sheand Resistance of CVD Graphene by Thionyl Chloride Chemical Doping. *Carbon*, **170**, 75-84. https://doi.org/10.1016/j.carbon.2020.07.038

[22] Khrapach, I., *et al.* (2012) Novel Highly Conductive and Transparent Graphene-Based Conductors. *Advanced Materials*, **24**, 2844-2849. https://doi.org/10.1002/adma.201200489

[23] Tareki, A.M., Lindquist, R.G., Kim, W., Heimbeck, M.S. and Guo, J. (2017) Terahertz Transparent Electrode Using Tripod Mandal Aperture Array. *IEEE Transactions on Terahertz Science and Technology*, **7**, 80-85.

[24] Wageh, S., *et al.* (2021) Silver Nanowires Digital Printing for Inverted Flexible Semi-Transparent Solar Cells. *Advanced Engineering Materials*, **23**, Article 2001305. https://doi.org/10.1002/adem.202001305

[25] He, W. and Ye, C. (2015) Flexible Transparent Conductive Films on the Basis of Ag Nanowires: Design and Applications: A Review. *Journal of Materials Science & Technology*, **31**, 581-588. https://doi.org/10.1016/j.jmst.2014.11.020

[26] De, S., *et al.* (2009) Silver Nanowire Nandworks as Flexible, Transparent, Conducting Films: Extremely High DC to Optical Conductivity Ratios. *ACS Nano*, **3**, 1767-1774. https://doi.org/10.1021/nn900348c

[27] Kim, S.H., Shin, H.J., Shin, K., Park, S.H. and Kim, D. (2013) Characterization of Flexible Hybrid Transparent Conductive Films Fabricated with Silver Nanowires and Carbon Nanotubes for Organic Solar Cells. 2013 *IEEE* 39*th Photovoltaic Specialists Conference* (*PVSC*), Tampa, FL, 16-21 June 2013, 2731-2733.

https://doi.org/10.1109/PVSC.2013.6745038

[28] Yasin, T. (2020) Optically Transparent Multifunctional Patch Antennas Integrated with Solar Cells for Small Satellites. Department of Electrical and Computer Engineering, Utah State University, Logan, UT84322.

[29] Garcia, P.A. (2014) Conception d'antennes optiquement transparentes pour stations de base. Thèse de doctorat en Électronique, télécommunications. http://www.theses.fr/2014NANT2096

[30] Martin, A., Castel, X., Himdi, M. and Lafond, O. (2017) Mesh Paramanders Influence on Transparent and Active Antennas Performance at Microwaves. *AIP Advances*, **7**, Article 085120. https://doi.org/10.1063/1.4985746

[31] Sa'ad, B.M., Rahim, S.K.A., Pander, T., Abedian, M. and Danesh, S. (2015) Transparent Microwave Crossover for Transparent *Butler matrix* Using Micro-Mandal Mesh Conductive Film. 2015 9*th European Conference on Antennas and Propagation* (*EuCAP*), Lisbon, 13-17 April 2015, 1.

[32] Rahim, S.K.A., Samingan, M.L. and Saady, B.M. (2016) Transparent Butler Matrix Using Micro-Mandal Mesh Conductive Film as a Conducting Element. 2016 *IEEE Asia-Pacific Conference on Applied Electromagnetics* (*APACE*), Langkawi, 11-13 December 2016, 105-108. https://doi.org/10.1109/APACE.2016.7915862